$C_{19}H_{26}O_5$: C, 68.24; H, 7.84. Found: C, 68.5; H, 7.6.

2,2-Bis(ethoxycarbonyl)-4-(acetoxymethyl)-1,2-dihydronaphthalene (3e′). ^{1}H-NMR: 1.26 (t, 6 H), 2.13 (s, 3 H), 3.43 (s, 2 H), 4.20 (q, 6 H), 5.05 (s, 2 H), 6.33 (s, 1 H), 7.25 (s, 4 H). MS: 346 (2), 213 (45), 185 (15), 169 (30), 141 (100), 129 (12), 115 (12), 43 (44). Anal. Calcd for $C_{21}H_{28}O_6$: C, 67.00; H, 7.50. Found: C, 66.9; H, 7.7.

2,2-Bis(ethoxycarbonyl)-3,4-diphenyl-1,2-dihydronaphthalene (3f). ^{1}H-NMR: 1.1 (t, 6 H), 3.79 (s, 2 H), 4.06 (q, 4 H), 6.82 (d, 1 H), 7.0–7.42 (m, 13 H). MS: 426 ($M^{\bullet+}$, 63), 380 (3), 353 (34), 307 (100), 281 (65), 203 (23). Anal. Calcd for $C_{30}H_{32}O_4$: C, 78.92; H, 7.06. Found: C, 78.8; H, 6.9.

2,2-Bis(ethoxycarbonyl)-3,4-diethyl-1,2-dihydronaphthalene (3g). ^{1}H-NMR: 1.28 (t, 6 H), 1.32 (t, 6 H), 2.50 (q, 2 H), 2.73 (q, 2 H), 3.50 (s, 2 H), 4.24 (q, 4 H), 7.22–7.50 (m, 4 H). MS: 330 ($M^{\bullet+}$, 10), 257 (31), 213 (25), 185 (100), 169 (42), 157 (51), 141 (37), 129 (76), 115 (19). Anal. Calcd for $C_{22}H_{32}O_4$: C, 73.30; H, 8.95. Found: C, 73.4; H, 9.1.

2,2,3,4-Tetrakis(ethoxycarbonyl)-1,2-dihydronaphthalene (3h). ^{1}H-NMR: 1.14–1.41 (m, 12 H), 3.52 (s, 2 H), 4.22 (m, 6 H), 4.42 (q, 2 H), 7.10–7.50 (m, 4 H). MS: 418 ($M^{\bullet+}$, 1), 373 (6), 299 (67), 225 (63), 199 (100), 154 (17), 127 (13), 115 (17). Anal. Calcd for $C_{24}H_{32}O_8$: C, 64.27; H, 7.19. Found: C, 64.3; H, 7.0.

2,2,4-Tris(ethoxycarbonyl)-3-methyl-1,2-dihydronaphthalene (3i). ^{1}H-NMR: 1.14 (t, 6 H), 2.44 (s, 3 H), 3.42 (s, 2 H), 3.77 (s, 3 H), 4.14 (m, 4 H), 7.10–7.35 (m, 3 H), 7.4–7.5 (m, 1 H). MS: 346 ($M^{\bullet+}$, 3), 241 (96), 227 (22), 213 (57), 201 (50), 169 (87), 157 (88), 142 (100), 128 (30), 115 (47), 59 (46). Anal. Calcd for $C_{22}H_{30}O_6$: C, 67.67; H, 7.74. Found: C, 67.5; H, 7.4.

2,2-Bis(ethoxycarbonyl)-3,4-di-*n*-propyl-1,2-dihydronaphthalene (3j). ^{1}H-NMR: 0.98 (m, 6 H), 1.17 (t, 6 H), 1.47 (m, 4 H), 2.26 (m, 2 H), 2.52 (m, 2 H), 3.33 (s, 2 H), 4.62 (q, 4 H), 7.03–7.27 (m, 4 H). MS: 358 ($M^{\bullet+}$, 15), 285 (46), 239 (29), 213 (39), 199 (53), 183 (48), 169 (33), 157 (60), 141 (75), 129 (100), 43 (84). Anal. Calcd for $C_{24}H_{36}O_4$: C, 74.19; H, 9.34. Found: C, 74.3; H, 9.1.

General Procedure for Competitive Experiments. Following the general procedure for reaction with Mn(III), a solution of **1** (2.15 mmol) and a few unsaturated substrates (for a total of 22 mmol) in AcOH (25 mL) were reacted in a thermostatic bath at 60 ± 5 °C for 12 h. The relative molar ratio of the competing unsatured substrates was varied for each couple in the range 1:1–1:10 as reported in Figure 1.

Generally, the conversion of the more reactive substrate was less than 15% in these conditions. The following couples were examined: (a) PhC≡CH/Me_3SiC≡CH; (b) PhC≡CPh/*n*-C_3H_7C≡C(*n*-C_3H_7); (c) PhC≡CH/*n*-$C_6H_{13}CH$=CH_2; (d) CH_2=CHCOOEt/HC≡CCOOEt; (e) *n*-$C_6H_{13}C$≡CH/HC≡CCOOEt; (f) *n*-$C_6H_{13}CH$=CH_2/Me_3SiC≡CH; (g) *n*-$C_6H_{13}CH$=CH_2/Et_3SiCH=CH_2; (h) HC≡CCH_2OH/PhC≡CPh; (i) *n*-$C_6H_{13}CH$=CH_2/*n*-$C_6H_{13}C$≡CH; (j) *n*-$C_6H_{13}CH$=CH_2/Me_3SiCH=CH_2; (k) *n*-$C_6H_{13}C$≡CH/HC≡CCH_2OH; (l) Me_3SiC≡CH/CH_2=$CHCH_2OH$; (m) *n*-$C_6H_{13}CH$=CH_2/*t*-PhCH=CHPh.

The results obtained as a mean of four independent experiments are plotted in Figure 1 with the limits of replication. Least-squares analysis of the experimental data gives the following relative rates: (a) 47 ± 3 (r = 0.9978); (b) 11.6 ± 0.4 (r = 0.991); (c) 10 ± 0.8 (r = 0.9985); (d) 9.7 ± 0.3 (r = 0.9995); (e) 5.3 ± 0.2 (r = 0.9998); (f) 4.6 ± 0.1 (r = 0.9991); (g) 4.1 ± 0.1 (r = 0.9955); (h) 3.4 ± 0.2 (r = 0.9992); (i) 3.0 ± 0.1 (r = 0.9995); (j) 2.4 ± 0.1 (r = 0.9990); (k) 2.8 ± 0.1 (r = 0.9996), (l) 1.1 ± 0.1 (r = 0.9987); (m) 2.5 ± 0.1 (r = 0.9990). These results allow us to obtain the absolute rate constants for the addition of malonyl radicals to unsaturated substrates reported in Table II.

Registry No. 1, 607-81-8; **2a**, 629-05-0; **2b**, 623-47-2; **2c**, 1066-54-2; **2d**, 536-74-3; **2e**, 107-19-7; **2f**, 501-65-5; **2g**, 928-49-4; **2h**, 762-21-0; **2i**, 23326-27-4; **2j**, 1942-45-6; **3a**, 141344-90-3; **3b**, 141344-91-4; **3c**, 141344-92-5; **3d**, 141344-93-6; **3e**, 141344-94-7; **3e′**, 141344-95-8; **3f**, 141344-96-9; **3g**, 141344-97-0; **3h**, 141344-98-1; **3i**, 141344-99-2; **3j**, 141345-00-8; *cis*-**7b**, 141345-01-9; *trans*-**7b**, 141345-02-0; *cis*-**7h**, 141345-03-1; *trans*-**7h**, 141345-04-2; *cis*-**7′h**, 141345-05-3; *trans*-**7′h**, 141345-06-4; Mn(III), 14546-48-6; PhCH=CH_2, 100-42-5; *n*-$C_6H_{13}CH$=CH_2, 111-66-0; Me_3SiCH=CH_2, 754-05-2; CH_2=$CHCH_2OH$, 107-18-6; CH_2=CHCOOMe, 96-33-3; (*E*)-PhCH=CHPh, 103-30-0; (*E*)-*n*-PrCH=CH-*n*-Pr, 14850-23-8; CH_2=C(Me)C(Me)=CH_2, 513-81-5; CH_2=CHCN, 107-13-1; CH_2=CHOAc, 108-05-4; CH_2=$CHCH_2C(O)OEt$, 1617-18-1; CH_2=C(Me)-*i*-Pr, 563-78-0; CH_2=$CHSiEt_3$, 1112-54-5; c-C_6H_{10}, 110-83-8; (*Z*)-EtOOCCH=CHCOOEt, 141-05-9; (*E*)-EtOOCCH=CHCOOEt, 623-91-6; (*Z*)-MeCH=CHMe, 590-18-1; MeC≡CMe, 503-17-3; HC≡CCOOMe, 922-67-8; $CH_2CHCOOEt$, 140-88-5.

Regioselectivity and Stereoselectivity in the Photodimerization of Rigid and Semirigid Stilbenes

Thomas Wolff,* Friedrich Schmidt, and Peter Volz

Universität Siegen, Fachbereich 8, D-5900 Siegen, FRG

Received April 14, 1992

The ($2\pi + 2\pi$)-photodimerizations of 2-phenylindene (**1**), 2-(4-methoxyphenyl)indene (**9**), and 5,10-dihydroindeno[2,1-*a*]indene (**2**) were investigated in a variety of homogeneous and micellar solvents. Four isomeric photodimers were formed from **1** and **9**: syn-head-to-tail, syn-head-to-head, anti-head-to-tail, and anti-head-to-head. Relative yields of these as well as syn/anti- and head-to-tail (ht)/head-to-head (hh) ratios were determined in various solvents and as a function of temperature. In **1** syn/anti ratios ranged from 1.07 to 1.62 and ht/hh ratios from 0.88 to 1.28. In **9** syn/anti ratios between 0.83 and 2.55 and ht/hh ratios between 0.4 and 1.2 were found; preferred formation of anti and hh products was observed in micellar solvents as expected from preorientation of reactants. Two photodimers (ht and hh) were found upon irradiation of **2**. ht/hh ratios ranged from 0.89 to 1.56. The variations of these ratios can be understood on the basis of a kinetic scheme, in which individual excimer states as precursors of the respective dimers are involved.

Introduction

Upon irradiation stilbene and its derivatives are known to undergo three different types of photoreactions: cis-trans isomerization,[1] and dihydrophenanthrene formation,[2] and dimerization.[3] Only the latter is possible when the central stilbene double bond is incorporated in a ring system, i.e., in rigid and semirigid stilbene compounds. Examples are 2-phenylindene (**1**) (semirigid) and 5,10-

(1) (a) Meier, H. In *Methoden der Organischen Chemie* (*Houben-Weyl*), Vol IV/5a, 4th ed.; Müller, E., Ed.; Thieme: Stuttgart, 1975; p 187. (b) Waldeck, D. H. *Chem. Rev.* **1991**, *91*, 415.

(2) Bromberg, A.; Muszkat, K. A.; Fischer, E. *Isr. J. Chem.* **1972**, *10*, 765.

(3) Lewis, F. D. *Adv. Photochem.* **1986**, *13*, 165.

0022-3263/92/1957-4255$03.00/0

Scheme I

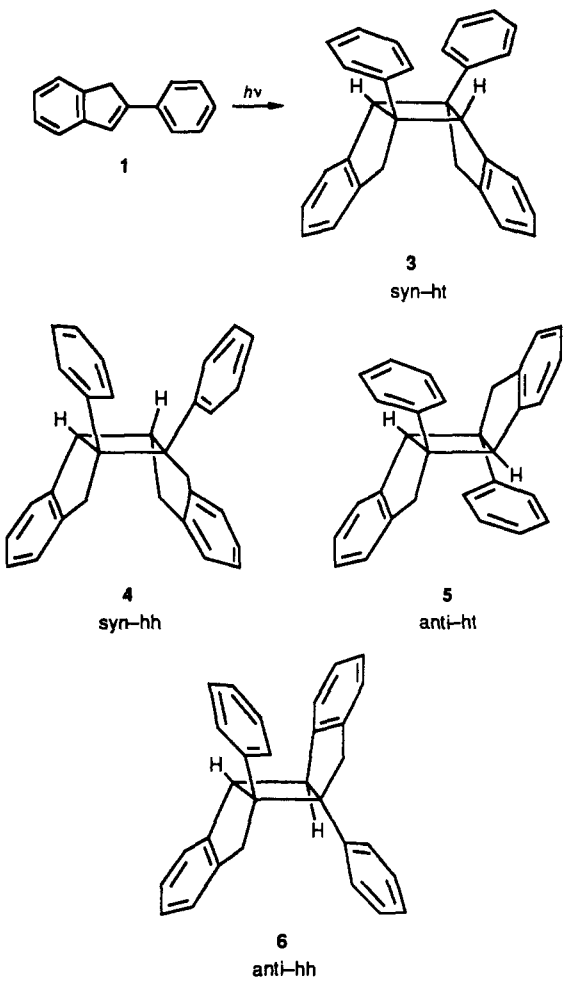

Scheme II

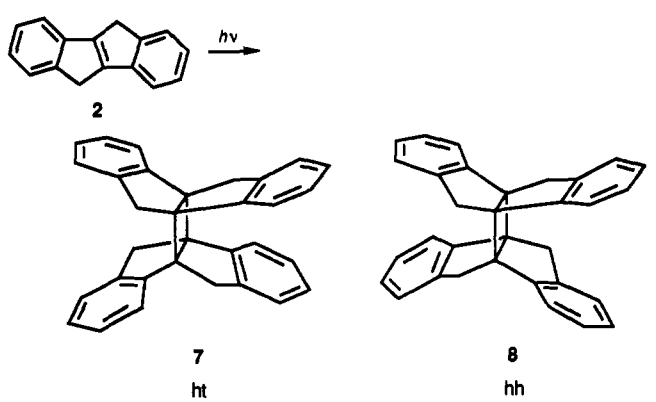

dihydroindeno[2,1-*a*]indene (2) (rigid).

Upon irradiation of 1 the formation of four isomeric photodimers can be expected: head-to-head (hh) and head-to-tail (ht) photodimers, both of which can exist in syn and anti (cis and trans) configuration as illustrated in Scheme I. The two possible photodimers of 2, i.e., the head-to-tail photodimer 7 and the head-to-head photodimer 8, have been described in the literature[4] (see Scheme II).

A widely accepted reaction sequence (not considering selectivity) for the photodimerization of *trans*-stilbenes arises from the diagram in Figure 1. It involves the excited singlet state of the stilbene, an excimer, and another ex-

(4) Shim, S. C.; Chae, J. S. *Bull. Chem. Soc. Jpn.* **1982**, *55*, 1310.

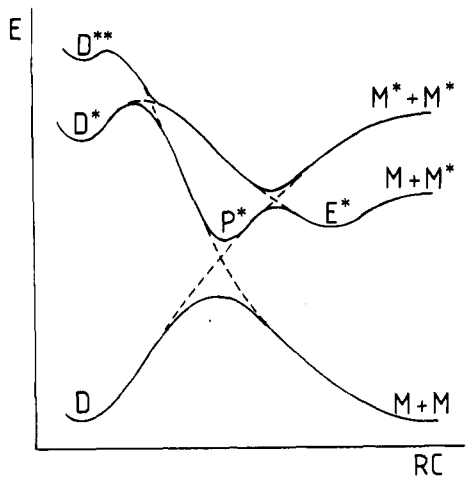

Figure 1. Schematic potential energy (*E*) surface diagram for photochemical ($2\pi + 2\pi$)-dimerizations, redrawn after Lewis[3] and Michl.[5] The reaction coordinate (RC) represents the distance between the centers of the monomers. D, dimer; E, excimer; M, monomer; P, pericyclic minimum.

cited intermediate, the so-called pericyclic minimum[3,5] (which is the consequence of avoided crossing of excited state surfaces). Applying this mechanism, Shim and Chae[4] derived a rate constant of excimer formation of 2.8×10^9 L mol^{-1} s^{-1} from quantum yield measurements. Moreover, the authors deduced a limiting quantum yield of 0.83 for dimer formation from the excimer state, and a ratio of product yields [7]:[8] = 2 was obtained after separation and recrystallization of the products.

In this paper we present the identification of the isomers 3–6 (scheme I) and an investigation of the selectivity of the photodimerizations of 1, 2, and a derivative of 1, 2-(4-methoxyphenyl)indene (9). Regio- and stereoselectivity

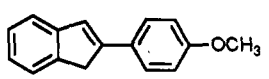

9

are shown to be sensitive to the choice of various homogeneous and micellar solvents as well as to the temperature.

Experimental Section

2-Phenylindene (1) was prepared via a literature procedure[6] from 2-indanone and 4-bromobenzene.

2-(4-Methoxyphenyl)indene (9). Dry 4-bromoanisole (0.5 g, 3 mmol) and 0.65 g (27 mmol) of dried (1 day at 130 °C) magnesium shavings were placed under an argon atmosphere in a dried apparatus consisting of a three-necked 100-mL flask, magnetic stirrer, gas inlet, mercury valve, reflux condensor, and 25-mL dropping funnel. A solution (2 mL) of 4.5 g (24 mmol) of bromoanisole in 10 mL of dry tetrahydrofuran was added. After being heated by means of a fan, the reaction started as indicated by a change of the color of the mixture. Then the remaining 8 mL of the bromoanisole solution was added dropwise under vigorous stirring whereby the solution kept boiling. After the addition the mixture was refluxed for 0.5 h. To this red-brown solution was added 3.57 g (27 mmol) of freshly recrystallized (from *n*-hexane) 2-indanone in 10 mL of absolute diethyl ether dropwise. A light flocky precipitate formed and the solution warmed up until the boiling temperature was reached. After the addition the mixture was refluxed for 2 h and then treated with 20 mL of half-concentrated hydrochloric acid. Eventually a colorless aqueous and an orange-yellow organic phase formed, which were separated. After drying the latter the organic solvent was

(5) Michl, J. *Photochem. Photobiol.* **1977**, *25*, 141.

(6) Plattner, P. A.; Sandrin, S.; Wyss, J. *Helv. Chim. Acta* **1946**, *29*, 1604.

evaporated. The remaining solid was dissolved in dry toluene and refluxed with 5 g (37 mmol) of $KHSO_4$ under an argon atmosphere. After filtration and evaporation of the toluene the product was recrystallized from acetic acid ethyl ester and sublimed in vacuo (0.01 Torr, 130 °C) to yield 3.53 g (16 mmol; 59%) of colorless plates of **9**: mp 211–213 °C; ^{1}H-NMR ($CDCl_3$) 3.78 ppm (s, 2 H), 3.85 (s, 3 H), 6.8–7.7 (m, 9 H); EI-mass spectrum *m/e* 222.2 (71.1), 149.0 (25.1), 83.1 (28.6), 81.1 (45.6), 71.1 (34.1), 69.1 (100), 55.7 (55.3), 55.1 (58.0), 43.1 (50.9), 40.1 (53.3).

2-(4-Hydroxyphenyl)indene (12). 2-(4-Methoxyphenyl)-indene (**9**) (2 g, 9 mmol) was dissolved in 100 mL of acetic acid containing 33% hydrobromic acid. The mixture was stirred and refluxed in an argon atmosphere for 24 h. After cooling, a suspension formed, which was made alkaline (employing concentrated sodium hydroxide solution) and filtered. Upon acidification of the filtered solution very small brown crystals of **12** precipitated, which were purified by two sublimations in vacuo (0.01 Torr, 160 °C) to give 0.29 g (1.4 mmol, 15%) of a light yellow powder: mp 219–222 °C dec; ^{1}H-NMR (CDCl) 3.74 ppm (s, 2 H), 6.7–7.7 (m, 10 H); EI-mass spectrum *m/e* 209.3 (15.8), 208.3 (100), 207.3 (50.3), 179.3 (11), 178.3 (20.5), 152.3 (9.7), 115.2 (11.4), 104.2 (8.1), 89.2 (11.2), 76.2 (8.5).

2-(4-(Dimethylamino)phenyl)indene (11). In an apparatus as used for the preparation of **9**, 0.61 g (25 mmol) of dried magnesium shavings and a few iodine crystals were heated to 100 °C. After evaporation of I_2 in vacuo, 0.5 g (2 mmol) of 4-bromo-*N*,*N*-dimethylaniline (Aldrich, purity 99%) was added in an argon atmosphere. Then 2 mL of a solution of 4.5 g (23 mmol) of 4-bromo-*N*,*N*-dimethylaniline in 10 mL of absolute tetrahydrofuran was rapidly added, and the solution was heated to boiling temperature by means of a fan. The start of the reaction was indicated by a slowly appearing brown solution color. Then the remaining 8 mL of the solution was added dropwise under vigorous stirring. The dropping was adjusted at such a speed that the solution kept boiling from the reaction heat. After the addition was completed the solution was refluxed for 0.5 h and allowed to cool to room temperature. Under an argon atmosphere 3.3 g (25 mmol) of 2-indanone (Aldrich, purity 98%) in 10 mL of dry tetrahydrofuran was added dropwise to the solution of the Grignard reagent, which thereby warmed up to boiling temperature again. After the addition the mixture was refluxed for 2 h. Then it was diluted with 20 mL of diethyl ether and hydrolyzed with 20 mL of half-concentrated hydrochloric acid. A light flocky solid formed at the organic/aqueous interface which was separated. Upon addition of concentrated sodium hydroxide solution to the aqueous phase (until alkaline reaction), a small amount of fine crystals formed which was filtered off and combined with the already separated solid. The combined solids were treated with 200 mL of boiling 2 M sodium hydroxide for 1 h. The solid was filtered off, washed with water, and dried over silica gel. After three recrystallizations from acetic acid ethyl ester 2.28 g (9.8 mmol, 39%) of large colorless plates of **11** was obtained: mp 255–257 °C dec; ^{1}H-NMR ($CDCl_3$) 2.98 ppm (s, 6 H), 3.73 (s, 2 H), 6.5–7.7 (m, 10 H); EI-mass spectrum *m/e* 234.6 (100), 233.6 (46.5), 190.6 (28.9), 188.6 (24.8), 116.7 (17.6), 56.5 (19.4), 42.5 (22.2), 40.5 (24.7), 17.5 (75.5), 16.3 (18.2).

5,10-Dihydroindeno[2,1-*a*]indene (2) was prepared as described in the literature[7] and showed the physical and spectroscopic properties reported there.

Homogeneous solvents (acetonitrile, benzene, 1-butanol, diethyl ether, isooctane, methanol) were purchased from Merck (Uvasol quality). The surfactants cetyltrimethylammonium bromide (Fluka) and chloride (Henkel) and dodecyltrimethylammonium bromide (Kodak) were recrystallized from acetone/methanol (10:1 mixture). Triply distilled water was used for preparing surfactant solutions.

Irradiations of up to 5 mM solutions of **1**, **2**, **9**, **10**, and **11** were performed under an argon atmosphere in a falling film apparatus employing a 125-W high pressure mercury lamp (Philips HPK) at wavelengths > 300 nm (Solidex-glass filtered). Quantum yields were obtained using the Hatchard–Parker procedure.[8] Samples

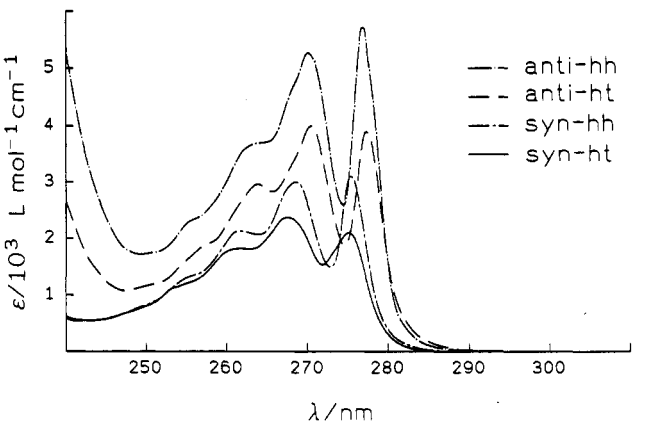

Figure 2. UV absorption spectra (absorption coefficient ϵ vs wavelength λ) of the four isomeric photodimers of 2-phenylidene (**1**) in isooctane at 25 °C.

and Parker's solution were irradiated through the gas/liquid interface at 25 °C.

For HPLC analyses and semipreparative HPLC separation of photoproducts a Knauer chromatograph was employed which was fitted with 250-mm × 4-mm and 250-mm × 16-mm columns (for analytic and semipreparative purposes, respectively) and coupled to an UV detector (Shimadzu Chromatopac OR 3A). The columns were filled with Lichrospher Si 100 (5 μm; Merck); *n*-heptane (Fluka, HPLC quality) served as the eluent. Analytical chromatograms were run at a pressure of 130 bar and a flow rate of 2 mL/min, semipreparative chromatograms at 40 bar and 8 mL/min.

A Beckman Acta M VII spectrophotometer, a Varian MAT 112 mass spectrometer, and a Spex fluorolog II were employed for measuring UV spectra, mass spectra, and fluorescence spectra. ^{1}H-NMR spectra were measured on Bruker WP 80 (80 MHz) or Bruker AC 200 (200 MHz) spectrometers. For analyzing ^{13}C-satellite signals spectra taken on a Bruker WH 400E (400 MHz) spectrometer were used.

Fluorescence lifetimes were derived from fluorescence decay curves measured after excitation by 337-nm subnanosecond pulses of a N_2 laser (Lambda Physik, Model K50 PS). Decay curves were recorded on a Hewlett-Packard digital oscilloscope (Model 54502 A) employing an Avalanche photodiode (Opto Electronics, Model PD 30) as a detector.

Viscosities were measured using Ostwald viscometers unless data were available in the literature.[9]

Results

(1) 2-Phenylindene (1). Assignment of Isomeric Photoproducts. Irradiated solutions of 2-phenylindene (**1**) were subjected to high pressure liquid chromatography (HPLC). Besides the educt peak, four product peaks appeared in the chromatograms. After separation by means of semipreparative HPLC the four products were analyzed using mass spectrometry, as well as UV and NMR spectroscopy. The UV spectra of the separated photoproducts are shown in Figure 2. They exhibit absorption at wavelengths < 290 nm only, in keeping with the structures of the dimers **3**–**6** in Scheme I. In the mass spectra of two of the products a small peak of the dimer molecular mass 384 was found. The peaks of the spectra were similar to those of the spectrum of **1**, indicating efficient splitting of the dimers into monomers inside the mass spectrometer. The other two products also gave spectra widely agreeing with that of the educt but no peak at masses exceeding the molecular mass peak of the educt were revealed.

(7) Saltiel, J.; Shannon, P. T.; Zafiriou, O. C.; Uriarte, A. K. *J. Am. Chem. Soc.* **1980**, *102*, 6799.

(8) Hatchard, C. G.; Parker, C. A. *Proc. R. Soc. London, Ser. A* **1956**, *235*, 518.

(9) (a) *Handbook of Chemistry and Physics*, 67th ed.; Weast, A. C., ed.; CRC Press: Boca Raton, FL, 1987. (b) *Landolt-Börnstein, Zahlenwerke und Funktionen aus Physik, Chemie, Astronomie, Geophysik und Technik*, Vol. IV/5a; Borchers, H., Hausen, H., Hellwege, K.-H., Schäfer, K., Schmidt, E., Eds.; Springer: Berlin, 1969.

Table I. ^{1}H-NMR Spectral Data of the Cyclobutane Protons of the Photodimers of 2-Phenylindene in $CDCl_3$ (cf. Scheme I)

dimer	δ/ppm	$^1J(^{13}C,^1H)$/ Hz	$^3J(^1H,^1H)$/ Hz	$^4J(^1H,^1H)$/ Hz
syn-hh 4	4.68	140	8.8	
anti-hh 6	4.12	140	3.3	
syn-ht 3	4.47	140		0.9
anti-ht 5	4.61	140		0

Obviously, these two photodimers are so labile that they split upon transfer to the gas phase so that the molecular mass peaks do not appear in the spectra. It turned out after the NMR analyses (see below) that the latter two isomers are the dimers in which the two phenyl rings are attached to neighboring C atoms of the cyclobutane ring of the dimers, i.e., the head-to-head dimers 4 and 6 in Scheme I. These two dimers can be expected to be less stable than the other two due to steric repulsion of the phenyl rings.

As revealed by UV absorption spectra and HPLC analyses, all the photodimers of 1 split into monomers upon irradiation at 254 nm in a clean photoreaction (except for the syn-hh dimer, which produced some side products which were not investigated further). This behavior is in keeping with the cyclobutane structure of the dimeric photoproducts given in Scheme I.

^{1}H-NMR spectra of the products exhibit peaks in three distinct ppm regions: 3–4 ppm (benzylic H), 4–5 ppm (cyclobutane H), and 6.5–7.5 ppm (aromatic H). Data of the cyclobutane protons are collected in Table I. Coupling of these protons cannot be observed because of their chemical equivalence. However, when one of the two cyclobutane protons is accidentally bound to a ^{13}C atom, coupling of the nuclear spins of hydrogen and ^{13}C occurs at a coupling constant of 140 Hz, giving rise to ^{13}C-satellite signals. These may be further split due to coupling with nuclear spins of hydrogen atoms bound to neighboring C atoms, since the chemical equivalence of the cyclobutane protons is remote in molecules with one ^{13}C–H bond. Assignment of products 3 to 6 was therefore made via an analysis of the splitting of the ^{13}C-satellite signals:[10,11] the largest coupling constant of 8.8 Hz is attributed to the syn-hh isomer 4 in which the two cyclobutane protons are bound to neighboring C atoms and the two C–H bonds form a dihedral angle of ca. 14°. A smaller coupling constant can be expected for the anti-hh dimer 6 in which a dihedral angle of ca. 104° for two cyclobutane protons is predicted from model calculations.[12] We therefore assign the isomer exhibiting 3.3-Hz coupling as the anti-hh dimer. In the two remaining compounds coupling between the two cyclobutane protons has to occur through-space and can be expected only in the syn-ht dimer 3 in which the four bonds between the two protons assume the form of a W.[10,13] The isomer with the coupling constant J = 0.9 Hz is therefore assigned the syn-ht dimer 3 while the isomer exhibiting only the 140-Hz coupling must be the anti-ht dimer.

Selectivity. As illustrated in Scheme III the photodimers of 1 show stereo isomery as well as constitutional isomery, so that regio- as well as stereoselectivity may occur

Scheme III

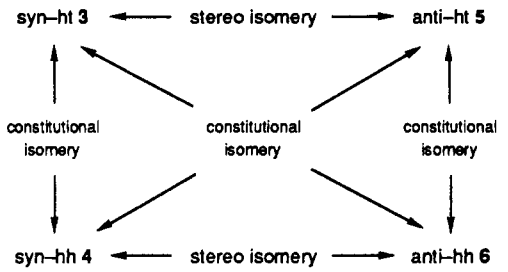

Table II. Relative Yields of the Formation of syn-ht, syn-hh, anti-ht, and anti-hh Photodimers of 2-Phenylindene (1), 2-(4-Methoxyphenyl)indene (9), and 5,10-Dihydroindeno[2,1-*a*]indene (2) in Various Solvents (homogeneous, homogeneous heavy atom, aqueous micellar) at 25 °C and syn/anti and ht/hh Ratios Which Are Reproducible within ±2%

solvent	syn-ht	syn-hh	anti-ht	anti-hh	syn/anti	ht/hh
2-Phenylindene (1)						
benzene	27.5	31.4	19.4	21.7	1.43	0.88
isooctane	29.4	29.9	20.7	20.0	1.46	1.00
2-propanol	30.4	26.7	25.4	17.5	1.33	1.26
1-bromobutane	25.2	26.6	27.3	21.0	1.07	1.10
0.2 M TBAI[a,b]	28.4	26.2	22.9	22.5	1.20	1.05
0.5 M DTAB[a,c]	30.9	25.4	25.3	18.4	1.29	1.28
0.5 M TTAB[a,c]	30.1	23.9	21.5	25.4	1.17	1.07
0.2 M CTAB[a,c]	27.6	28.7	20.2	23.4	1.29	0.92
2-(4-Methoxyphenyl)indene(9)						
acetonitrile	38.3	36.5	19.2	9.0	2.55	1.20
benzene	33.0	31.8	17.0	18.2	1.84	1.00
0.2 M CTAB[a,c]	23.8	21.7	4.8	49.7	0.83	0.40
5,10-Dihydroindeno[2,1-*a*]indene (2)						
acetonitrile						1.31
benzene						1.51
1-butanol						0.97
diethyl ether						1.56
isooctane						1.29
methanol						0.89
2-propanol						1.15
0.5 M DTAB[a,c]						1.25
0.5 M TTAB[a,c]						1.27
0.2 M CTAB[a,c]						1.07

[a] TBAI = tetrabutylammonium iodide; DTAB = dodecyltrimethylammonium bromide; TTAB = tetradecyltrimethylammonium bromide; CTAB = cetyltrimethylammonium bromide. [b] In 2-propanol. [c] In water.

in the photodimerization. Relative yields of isomers were determined from integrals of NMR signals of the cyclobutane protons and are listed in Table II together with ratios of the formation of syn and anti isomers (indicating stereoselectivity) and of head-to-tail (ht) and head-to-head (hh) isomers (indicating regioselectivity). In homogeneous organic solvents containing light atoms only, the stereoselectivity appears more pronounced as compared to homogeneous heavy atom solvents and to aqueous micellar media (which are heavy atom solvents, too, due to the presence of bromide counterions at high local concentrations near the solubilized photoeducts). The stereoselectivity can be varied but not inverted by changing the solvent. The regioselectivity, however, can be directed by choosing the solvent in such a way that either ht or hh dimer formation prevails.

The quantum yield of photodimerization decreases in heavy atom solvents: as compared to 2-propanol the relative quantum yield at 25 °C is 79% in 1-bromobutane and 41% in propanol/0.2 M tetrabutylammonium iodide. This indicates that the photodimerization proceeds via the excited singlet state of 1 (the fluorescence lifetime of 1 in isooctane was found to be 1.6 ns; see Table V). Absolute values of the dimerization quantum yields are given in Table III. The dependence of the quantum yield on

(10) Günther, H. *NMR-Spektroskopie*, 2nd ed.; Thieme: Stuttgart, 1979.
(11) Williams, D. H.; Flemming, I. *Spektroskopische Methoden zur Strukturaufklärung*, 4th ed.; Akademie: Berlin, 1977.
(12) Höweler, U. *MOBY-molecular modelling on PC*, version 1.4; Springer: Berlin 1991.
(13) Zschunke, A. *Kernmagnetische Resonanzspektroskopie in der Organischen Chemie*, 2nd ed.; Akademie: Berlin, 1977.

Table III. Quantum Yields Φ_D of Photodimerization (last digits vary by ±3) in Various Solvents at 25 °C As Compared with Solvent Viscosities (c_M, monomer concentration)

solvent	Φ_D	η/(mPa·s)
2-Phenylindene (1) (c_M = 2.5 mmol/dm^3)		
benzene	0.00371	0.606
0.2 M CTAB	0.0189	1.56
isooctane	0.0284	0.484
2-propanol	0.0131	2.05
5,10-Dihydroindeno[2,1-*a*]indene (2) (c_M = 1 mmol/dm^3)		
acetonitril	0.0157	0.345
benzene	0.0077	0.606
1-butanol	0.0075	2.60
0.2 M CTAB	0.0181	1.56
diethyl ether	0.0182	0.222
isooctane	0.0154	0.484
methanol	0.0157	0.547
2-propanol	0.00938	2.05

monomer concentration was investigated in isooctane: Figure 3 depicts a plot of reciprocal quantum yield versus reciprocal monomer concentration. The plot is linear, exhibiting a slope of 0.0842 mol/dm^3 and an intersect with the y axis of 5.21, which corresponds to an extrapolated dimerization quantum yield at infinite concentration of $\phi_{D,\infty}$ = 0.192.

The temperature dependence of selectivity was investigated in two solvents: isooctane and 2-propanol. As revealed by the data in Table IV, syn/anti ratios decrease as the temperature increases. ht/hh ratios also decrease with increasing temperature in 2-propanol, while the values in isooctane pass through a minimum.

(2) 2-(4-Methoxyphenyl)indene (9). Upon irradiation of 2-(4-methoxyphenyl)indene (**9**), four photodimers are formed analogously to the photodimerization of **1**. As compared to the photoproducts of **1**, chemical shifts of the NMR signals of the cyclobutane protons are slightly changed (syn-ht, 4.35 ppm; syn-hh, 4.57 ppm; anti-ht, 4.49 ppm; anti-hh, 4.04 ppm; all in $CDCl_3$; cf. Table I). High selectivities can be achieved when **9** is photodimerized in homogeneous and in micellar media. The data in Table II show that in acetonitrile as well as in benzene preferred formation of syn photodimers takes place, while in 0.2 M CTAB anti photodimer formation predominates and a high excess of hh products is formed.

(3) 2-(4-(*N*,*N*-Dimethylamino)phenyl)indene (10) and 2-(4-Hydroxyphenyl)indene (12). These two derivatives did not form photodimers upon irradiation. In the case of **10**, changes in the emission properties appeared when the solvent polarity was varied: increasing polarity gave rise to a significant red shift of the emission maximum, while the quantum yield decreased and the fluorescence lifetime increases (Table V). These features might indicate the formation of an excited TICT (twisted

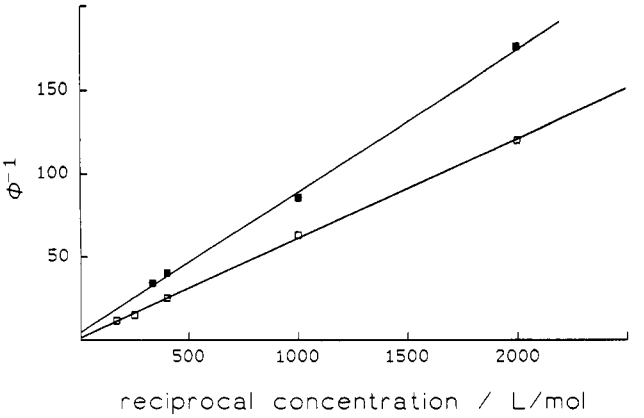

Figure 3. Plots of reciprocal dimerization quantum yield ϕ^{-1} vs reciprocal monomer concentration in isooctane at 25 °C. (■) 2-phenylindene (**1**), (□) 9,10-dihydroindeno[2,1-*a*]indene (**2**).

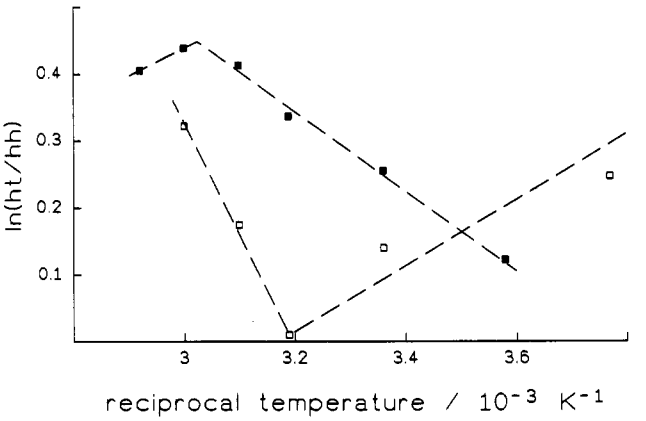

Figure 4. Logarithmic dependence of the ratio of the yields of isomeric photodimers of 9,10-dihydroindeno[2,1-*a*]indene ln (ht/hh) on reciprocal temperature (■) in isooctane, (□) in 2-propanol.

Table IV. Temperature Dependence of Product Distributions and of Ratios of Syn/Anti and ht/hh Dimer Production. Ratios Can Be Reproduced within ±2%

solvent	temp/°C	syn-ht	syn-hh	anti-ht	anti-hh	syn/anti	ht/hh
2-Phenylidene (1)							
isooctane	−22	33.7	28.0	22.2	15.9	1.62	1.27
isooctane	25	29.4	29.9	20.7	20.0	1.46	1.00
isooctane	35	28.6	27.3	23.7	20.5	1.26	1.09
isooctane	50	29.5	25.8	23.8	20.9	1.24	1.14
isooctane	70	28.4	25.7	23.5	22.3	1.18	1.08
2-propanol	25	30.4	26.7	25.4	17.5	1.33	1.26
2-propanol	35	29.8	26.2	24.1	19.8	1.28	1.17
2-propanol	50	28.4	27.2	24.3	20.0	1.26	1.12
2-propanol	60	27.8	27.2	24.8	20.1	1.22	1.11
5,10-Dihydroindeno[2,1-*a*]indene (2)							
isooctane	7						1.13
isooctane	25						1.29
isooctane	40						1.40
isooctane	50						1.51
isooctane	60						1.55
isooctane	70						1.50
2-propanol	−8						1.28
2-propanol	25						1.15
2-propanol	40						1.01
2-propanol	50						1.19
2-propanol	60						1.38

Table V. Fluorescence Lifetimes of 2-Phenylindene (1), 5,10-Dihydroindeno[2,1-*a*]indene (2), and 2-(4-(*N*,*N*-Dimethylamino)phenyl)indene (10) at c = 0.1 mmol/dm³ and at 25 °C in Various Solvents

substance	solvent	lifetime/ns
1	isooctane	(1.6 ± 0.2)
2	isooctane	(1.9 ± 0.2)
10	isooctane	(1.8 ± 0.2)
10	acetonitrile	(2.3 ± 0.2)

Table VI. Rate Constants k_d of the Photodimerization of 2 as Compared to Calculated Maximum Rate Constants $k_{d,m}$ at Various Temperatures T and Corresponding Viscosities[6] η in Isooctane

T/K	η/mPa·s	$\Delta\Phi_D^{-1}/\Delta C_M^{-1}$/ mmol/L	$k_d/10^9$ dm³ mol⁻¹ s⁻¹	$k_{d,m}/10^9$ dm³ mol⁻¹ s⁻¹
298	0.484	59.8	8.4	14
303	0.452	68.5	7.3	15
313	0.404	97.2	5.1	17

intramolecular charge transfer) state[14] which is uncapable of forming dimers.

(4) 5,10-Dihydroindeno[2,1-*a*]indene (2). Upon irradiation of millimolar solutions of 5,10-dihydroindeno-[2,1-*a*]indene (2) in various solvents, two products were formed. These are—according to HPLC chromatograms and to ^{1}H-NMR spectra—the head-to-tail (ht) and the head-to-head (hh) stereoisomers of the photodimer of 2 (cf. Scheme II). Measured ht/hh ratios in different solvents are collected in Table II. Inspection of the table reveals that the excess ht production is highest in solvents of medium polarity such as benzene or diethyl ether while in highly polar solvents the formation of hh dimers can slightly prevail. The value ht/hh = 1.51 in benzene can be taken as resembling the literature value ht/hh = 2 within the accuracy given by the authors.[4] The product ratio is independent of the monomer concentration and of the degree of photoconversion. Irradiation of the solid educt in aqueous suspension does not lead to photodimerization.

Dimerization quantum yields $\phi_D = \phi_{ht} + \phi_{hh}$ increased as a function of concentration. Plots of reciprocal dimerization quantum yield versus reciprocal monomer concentration c_M (cf. Figure 3) gave straight lines according to

$$\phi_D^{-1} = (\tau_M \cdot k_r)^{-1} \cdot c_M^{-1} + \phi_{D,\infty}^{-1} \quad (1)$$

Slopes of such plots determined in isooctane at three temperatures are listed in Table VI together with dimerization rate constants k_r calculated from eq 1 using a monomer lifetime (τ_M) of 1.9 ns (Table V), which can be taken as independent of temperature since the fluorescence quantum yield does not change within this temperature range.[15] The quantum yield at infinite monomer concentration is $\phi_{D,\infty}$ = 0.57.

The temperature dependence of the ht/hh ratio was studied in isooctane and 2-propanol as solvents. Data are given in Table IV (cf. Figure 4). In isooctane the ratio passes through a maximum and in 2-propanol through a minimum as a function of temperature.

Both the dimers can be split into monomers upon irradiation at 254 nm with quantum yields of 0.16 and 0.31 for the ht and the hh dimer, respectively (measured in isooctane at 25 °C starting with a dimer concentration of 0.429 mmol/L).

Discussion

The observed increase of regio- and stereoselectivity upon performing irradiations of 9 in micellar solutions can be ascribed to preorientation of the monomers solubilized in the micelles (similar to observations in the photodimerization of polar substituted anthracenes[16,17]): an orientation of the polar substituent towards the water phase and of the less polar indene moiety of the monomer towards the micellar core is likely, and dimerization of molecules oriented in this way leads to the formation of hh dimers (cf. Table II). However, the preferred orientation of the long axis of the molecule seems to be not strictly radial, since more anti-hh dimers than syn-hh dimers are formed.

Less obvious is the origin of the selectivity in the dimerization of the nonpolar compounds 1 and 2 in homogeneous solvents. The temperature dependence of the selectivity (Table IV) suggests a kinetic reason. Therefore, an understanding of the observed effects will depend on a justified kinetic scheme describing the dimerization process. Previously,[4] the intermediacy of a common excimer state in the formation of both the dimers of 2 was postulated. This cannot account for the results since once an intermediate excimer is formed, the geometry of the product is fixed. An equilibration of ht and hh excimers (as in the dimerization of anthracene derivatives[18]) cannot take place since changing from hh to ht excimer geometry is only possible via the rotation of one monomer about an axis within the molecular plane, thus interrupting the overlap of π-systems. Also, a common 1,4-biradical intermediate, in which only three bonds of the cyclobutane ring are formed, cannot lead to both the dimers. (1,4-Biradicals are frequently discussed as intermediates in triplet ($2\pi + 2\pi$)-photocycloaddition reactions of enones and alkenes.[19])

On the other hand, the involvement of excited intermediates is suggested from three independent observations: (i) In Table VI dimerization rate constants k_d are listed at three temperatures together with corresponding solvent viscosities and maximum rate constants $k_{d,m}$, which were calculated for a diffusion-controlled process according to

$$k_{d,m} = 16\pi N_A \cdot r_M \cdot D_M \quad (2)$$

where N_A is Avogadro's number and r_M and D_M are radius and diffusion constant of the monomer 2. D_M was estimated from the Stokes–Einstein relation (assuming identical $r_M \approx 0.25$ nm in (2) and (3)), where k is the Boltzmann

$$D_M = kT/(6\pi\eta r_M) \quad (3)$$

constant. Contrary to the calculated rate constants, k_d decreases with increasing temperature. This indicates a mechanism involving intermediates such as excimers which can revert to the monomers. (ii) Product ratios as a function of temperautre (Table IV) exhibit extrema which are distinct for the solvents used. If

$$\phi_{ht}/\phi_{hh} = ht/hh = k_{ht}/k_{hh} \quad (4)$$

where ϕ_i and k_i (i = ht or hh) represent quantum yields

(14) Rettig, W. *Angew. Chem., Int. Ed. Engl.* **1986**, *25*, 971.
(15) Saltiel, J.; Zafiriou, O. C.; Megarity, E. D., Lamola, A. E. *J. Am. Chem. Soc.* **1968**, *90*, 4759.
(16) Wolff, T. *J. Photochem.* **1981**, *16*, 343.
(17) Wolff, T.; Müller, N. *J. Photochem.* **1983**, *23*, 131.
(18) Wolff, T. *Z. Naturforsch. A* **1985**, *40*, 1105.
(19) (a) Hastings, D. J.; Weedon, A. C. *J. Am. Chem. Soc.* **1991**, *113*, 8525. (b) Becker, D.; Haddad, N.; Sahali, Y. *Tetrahedron Lett.* **1989**, *30*, 2661.

Scheme IV[a]

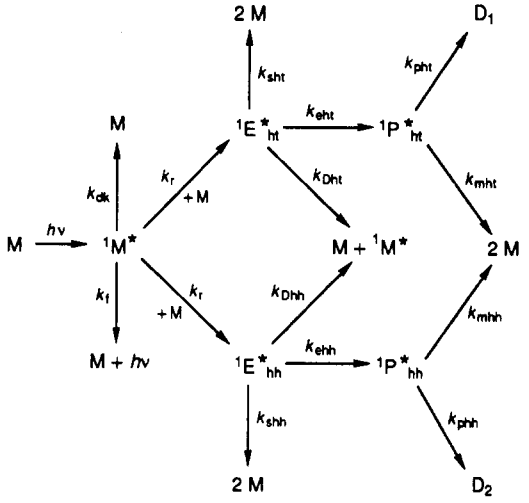

[a] M = ground state monomer; $^1M^*$ = singlet excited monomer; $^1E^*_i$ = excimer precursor of dimer i; $^1P^*_i$ = pericyclic minimum on the excited state surface; D_i = photodimer; k_{dk} = rate constant of dark (radiationless) decay of monomers; k_f = rate constant of monomer fluorescence; k_{ri} = rate constant of excimer formation; k_{si} = rate constant of radiationless (diabatic) split of excimers; k_{Di} rate constant of adiabatic excimer dissociation; k_{ei} = rate constant for formation of pericyclic minimum; k_{pi} = rate constant of dimer formation from $^1P^*_i$; k_{mi} = rate constant of formation of monomers from $^1P^*_i$; i = ht or hh.

and overall rate constants for the formation of individual dimers

$$^1M^* + M \rightarrow D_i \quad (5)$$

k_i can be expressed as

$$k_i = k^\circ_i \exp(\Delta S_i^\#/R - \Delta H_i^\#/RT) \quad (6)$$

Here, $\Delta S_i^\#$ and $\Delta H_i^\#$ are Eyring's entropy and enthalpy of activation, respectively, and R is the gas constant. In the photodimerization of **2** a plot of ln (ht/hh) vs reciprocal temperature should yield a straight line according to

$$\ln(\phi_{ht}/\phi_{hh}) = \ln(ht/hh) = \ln(k_{ht}/k_{hh}) = \ln(k_{ht}^\infty/k_{hh}^\infty) + \Delta S_{ht}^\#/R - \Delta H_{ht}^\#/RT - \Delta S_{hh}^\#/R + \Delta H_{hh}^\#/RT \quad (7)$$

Contrary to this expectation, Figure 4 shows that an inversion of the slope of such plots occurs in isooctane and 2-propanol as solvents, which is only possible when distinct intermediates are considered. Inversions of the temperature dependence of regio- or stereoselectivity were observed previously in a variety of bimolecular triplet reactions leading to oxetanes.[20] (iii) Without intermediates being involved, the extrapolated dimerization quantum yields at infinite monomer concentration $\phi_{D,\infty}$ should be unity. Figure 3 reveals that this is not the case.

We are, therefore, prompted to discuss the dimer formation of **2** on the basis of Scheme IV involving individual excimer states as precursors of ht and hh dimers, respectively. We address the excited intermediates as excimers following the evidence given in previous studies as comprized in Lewis' review article.[3] However, as we do not have specific experimental proof for excimers (such as excimer emission) in our systems, we cannot exclude other possible structures of the excited intermediates (such as 1,4-biradicals).

According to Scheme IV, we can express the lifetimes of the excited states as

$$\tau_M = (k_f + k_{dk})^{-1} \text{ (since } k_r[M] < (k_f + k_{dk}), \text{ cf. Table VI)} \quad (8)$$

$$\tau_{Eht} = (k_{sht} + k_{Dht} + k_{eht})^{-1} \quad (9)$$

$$\tau_{Ehh} = (k_{shh} + k_{Dhh} + k_{ehh})^{-1} \quad (10)$$

$$\tau_{Pht} = (k_{pht} + k_{mht})^{-1} \quad (11)$$

$$\tau_{Phh} = (k_{phh} + k_{mhh})^{-1} \quad (12)$$

Assuming that diffusion is rate determining for excimer formation, the k_{ri} are identical

$$k_{rht} = k_{rhh} = k_r \quad (13)$$

Assuming further quasi-stationarity for the concentrations of $^1M^*$, $^1E^*_i$, and $^1P^*_i$, kinetic expressions for the concentrations of excited state molecules can be derived which can be used to describe the monomer decay

$$-(dc_M/dt) = [2I_A k_r c_M(k_{eht}\tau_{Eht}k_{pht}\tau_{Pht} + k_{ehh}\tau_{Ehh}k_{phh}\tau_{Phh})]/[\tau_M^{-1} + k_r c_M((k_{sht} + k_{eht})\tau_{Eht} + (k_{shh} + k_{ehh})\tau_{Ehh})] \quad (14)$$

(I_A is the rate of consumption of photons by the monomer in mol/(Ls)). The reciprocal of the overall dimerization quantum yield

$$\phi_D = -(dc_M/dt)/2I_A \quad (15)$$

depends linearly on the reciprocal monomer concentration

$$\phi_D^{-1} = [(k_{sht} + k_{eht})\tau_{Eht} + (k_{shh} + k_{ehh})\tau_{Ehh}]/(k_{eht}\tau_{Eht}k_{pht}\tau_{Pht} + k_{ehh}\tau_{Ehh}k_{phh}\tau_{Phh}) + [\tau_M^{-1}/(k_r(k_{eht}\tau_{Eht}k_{pht}\tau_{Pht} + k_{ehh}\tau_{Ehh}k_{phh}\tau_{Phh}))]\cdot c_M^{-1} \quad (16)$$

This expression describes a plot of reciprocal dimerization quantum yield vs monomer concentration (Figure 3). The first term on the right side of eq 16 represents the quantum yield at infinite monomer concentration, while the slope is expressed by the factor of c_M^{-1} in the second term. Probabilities for the formation of a dimer from the corresponding excimer via the respective pericyclic minimum are given by

$$P_{ht} = k_{eht}\tau_{Eht}k_{pht}\tau_{Pht} \quad (17)$$

and

$$P_{hh} = k_{ehh}\tau_{Ehh}k_{phh}\tau_{Phh} \quad (18)$$

The sum of these probabilities can be derived from the slope of the plot shown in Figure 3 which is given in Table VI:

$$P_{ht} + P_{hh} = 1/[k_r\tau_M(\Delta\phi_D^{-1}/\Delta c_M^{-1})] \quad (19)$$

With the data of Tables V and VI the sum amounts to 0.61.

Since product ratios ht/hh are independent of monomer concentration and of reaction progress, they can be taken as quantum yield ratios

$$\phi_{ht}/\phi_{hh} = ht/hh = P_{ht}/P_{hh} = (k_{eht}\tau_{Eht}k_{pht}\tau_{Pht})/(k_{ehh}\tau_{Ehh}k_{phh}\tau_{Phh}) \quad (20)$$

and with the known value of the overall dimerization quantum yield $\phi_D = 0.0154$ (in isooctane at 25 °C for a starting monomer concentration of 1 mol/L; Table III) and the corresponding ratio ht/hh = 1.29 (Table II), individual

(20) (a) Pelzer, R.; Scharf, H.-D.; Buschmann, H. *Chem. Ber.* **1989**, *122*, 1187. (b) Buschmann, H.; Scharf, H.-D.; Hoffmann, N.; Plath, M. W.; Runsink, J. *J. Am. Chem. Soc.* **1989**, *111*, 5367. (c) Buschmann, H.; Scharf, H.-D.; Hoffmann, N.; Esser, P. *Angew. Chem., Int. Ed. Engl.* **1991**, *30*, 477.

quantum yields and probabilities can be calculated

$$\phi_{ht} = \phi_D/(1 + hh/ht) = 0.00868 \quad (21)$$

$$\phi_{hh} = \phi_D/(1 + ht/hh) = 0.00672 \quad (22)$$

$$P_{ht} = 0.61/(1 + hh/ht) = 0.34 \quad (23)$$

$$P_{hh} = 0.61/(1 + ht/hh) = 0.27 \quad (24)$$

Using extrapolated dimerization quantum yields at infinite monomer concentration $\phi_{D,\infty}$, we arrive at limiting individual quantum yields of $\phi_{ht,\infty} = 0.32$ and $\phi_{hh,\infty} = 0.25$ which are close to P_{ht} and P_{hh}, indicating that at high monomer concentration almost every excited monomer is deactivated via excimers.

The most likely step of the reaction mechanism in which selectivity can be introduced is the adiabatic dissociation of excimers (k_{Di}) leading to an excited and a ground state monomer. These may subsequently form a rearranged excimer. While the monomers for this latter process predominantly stem from the most labile of the original excimers, the secondary excimers will be formed at the same hh/ht ratio as the original ones. Thereby the product ratio is affected.

The numerator of the first term on the right side of eq 16 represents the sum of the probabilities for diabatic decay of excimers, i.e., radiationless deactivation and formation of dimers. If we multiply the intersection of the plot in Figure 3 with the y axis by ($P_{ht} + P_{hh}$), the sum of the diabatic excimer decay probabilities becomes

$$(k_{sht} + k_{eht})\tau_{Eht} + (k_{shh} + k_{ehh})\tau_{Ehh} = 1.76 \times 0.61 = 1.07 \quad (25)$$

The combined sums of the probabilities for diabatic and adiabatic excimer decay yield 2. Therefore the sum of the probabilities for adiabatic decay amounts to

$$k_{Dht}\tau_{Eht} + k_{Dhh}\tau_{Ehh} = 2 - 1.07 = 0.93 \quad (26)$$

Individual probabilities cannot be derived. However, the quite high value of 0.93 for the sum indicates that the adiabatic excimer decay can be responsible for introducing selectivity. Thus, the stability of the excimers against adiabatic dissociation might be the quantity influenced by solvent changes and temperature, giving rise to the observed dependence of selectivity on these parameters. The observation that heavy atom solvents reduce quantum yields *and* selectivity is now understood since heavy atoms can interact with any excited singlet state in Scheme IV (leading to nonreacting triplet states), thus diminishing the probability of formation of rearranged excimers.

Table VII. Limiting Quantum Yields $\Phi_{Di,\infty}$ (i = ht or hh) at Infinite Monomer Concentrations in Isooctane at 25 °C for the Photodimerization of 2-Phenylindene (1) and 9,10-Dihydroindeno[2,1-*a*]indene (2) and Probabilities P_i for the Formation of Dimers from the Respective Excimers (see text)

dimer	$\Phi_{Di,\infty}$	P_i
2-Phenylindene (1)		
syn-ht **3**	0.056	0.16
syn-hh **4**	0.057	0.16
anti-ht **5**	0.039	0.11
anti-hh **6**	0.038	0.11
9,10-Dihydroindeno[2,1-*a*]indene (**2**)		
ht **7**	0.32	0.34
hh **8**	0.25	0.27

An analogous treatment of the results for the photodimerization of 2-phenylindene (1) (extending Scheme IV by two additional possible products) leads to the data in Table VII, where limiting quantum yields for the formation of individual dimers of 1 and corresponding dimer formation probabilities P_i are comprized and compared with the values for the dimerization of 2 discussed above. Inspection of the table reveals considerably smaller quantum yields for the dimerization of 1. The quotient $\phi_D/\Sigma P_i$ represents the fraction of excited monomers which forms excimers. This fraction amounts to 35% in the case of 1 and 93% in the case of 2. The greater flexibility of the 2-phenylindene molecule might slow down the efficiency of excimer formation.

Conclusions

Regio- and stereoselectivity in the photodimerization of 2-phenylindene and 9,10-dihydroindeno[2,1-*a*]indene may be directed by appropriately choosing solvent and reaction temperature. Suitable polar derivatives of 2-phenylindene may yield a high excess of anti-hh dimers in micellar environments. Quantum yield data suggest a reaction mechanism involving individual excimer precursors of the dimers.

Acknowledgment. Financial support by the Deutsche Forschungsgemeinschaft and by the Fonds der Chemischen Industrie is gratefully acknowledged. We thank Dr. F.-W. Grevels, Mülheim, and Dr. H. Uzar, Siegen, for valuable discussion.